



OPEN ACCESS

RECEIVED

9 September 2019

REVISED

24 December 2019

ACCEPTED FOR PUBLICATION

6 January 2020

PUBLISHED

23 January 2020

Original content from this work may be used under the terms of the [Creative Commons Attribution 4.0 licence](#).

Any further distribution of this work must maintain attribution to the author(s) and the title of the work, journal citation and DOI.



PAPER

Dynamic phase fluctuations in potential-driven Bose–Einstein condensate

Decheng Ma¹ , Vladimir Koval² and Chenglong Jia¹ ¹ Key Laboratory for Magnetism and Magnetic Materials of MOE, Lanzhou University, 730000 Lanzhou, People's Republic of China² Institute of Materials Research, Slovak Academy of Sciences, Watsonova 47, 04001 Kosice, SlovakiaE-mail: cljia@lzu.edu.cn**Keywords:** Bose–Einstein condensate, phase fluctuations, decoherent effect, multi-peak structure

Abstract

We report on the dynamics of a Bose–Einstein condensate in one and two dimensions driven by the time-dependent harmonic trapping potential. Without the inter-particle interaction, the condensate exhibits the coherent behavior with the time-oscillating density distribution. When the inter-particle interaction is taken into consideration, the phase fluctuations, the multi-peak structure of the density distribution, and the coherence revival phenomenon, apart from the well-studied density oscillation behavior, can be observed in the condensate. Furthermore, it is demonstrated that due to the dimensional restriction these effects are more stable in the two and three-dimensional system, if compared to the one-dimensional case.

1. Introduction

Phase coherence is a novel property of a Bose–Einstein condensate (BEC), which is important for metrology and quantum information applications [1–4]. However, the phase coherence property of BECs can be perturbed, or ultimately destroyed by phase fluctuations arising from various sources [5–20]. For instance, the thermal fluctuation [9–11], change of the trapping potential [18, 19], variance of the inter-particle interaction [6, 13] have been reported to suppress the phase coherence of BEC. By releasing from the trapping potential, the phase fluctuations can be transformed into density fluctuations, represented typically by a multi-peak distribution structure, which can be in turn used for the description of the phase fluctuations [16, 17].

On the other hand, the time-dependent harmonic trapped BECs exhibit an intrinsic conformal symmetry [21–23], where the widths of the condensate wave packet for different times can be linked to each other by the time-dependent scale parameters. Hence, with the aid of scale parameters, the condensates experiencing the time-dependent harmonic potentials can be transformed into time-independent forms of which the spatial variation of density widths can be inferred from the scale parameters [23–38]. The monopole, dipole and quadrupole collective dynamics of the condensate, the self-similar collapsing dynamics, and the expanding dynamics after switching off the trapping potential can all be well described by the scaling method [24, 31, 36, 38]. Kuznetsov *et al* [33] and Zakharov *et al* [36] have also demonstrated that the scaling method in the hydrodynamic limit can be used for describing the angular oscillations of differently shaped BECs and the oscillations at the edges of the expanding condensate. However, when the trapping potential varies fast or changes suddenly, the condensate cannot evolve adiabatically; large phase fluctuations may occur in the condensate, which could give rise to a multi-peak structure of the density distribution of the condensates, and ultimately would lead to the deterioration of the coherence of BEC [18, 31]. Such dynamic effects are clearly beyond capabilities of the scaling method. The origin of phase fluctuations in the time-dependent trapped BECs has not been fully understood and their effect on the phase coherence of the condensates needs to be investigated in detail.

In this paper, the phase fluctuations induced in a BEC by the time-dependent harmonic trapping potential are investigated. By using the algebraic dynamic approach and the scaling method in the ideal Bose gas limit with no inter-particle interaction, a comprehensive description of the condensate density variation with time is

provided and subsequently confirmed by numeric simulations. In the ideal Bose gas limit, the phase fluctuations are absent, and so the condensate remains coherent all the time, even the trapping potential changes very fast with time. If the inter-particle interaction is taken into account, the scaling method can provide a consistent description of the overall variation of the condensate driven by slowly (harmonically) changing potentials. However, additional multi-peak structure appears in the system due to the phase fluctuations induced by the fast time-increasing potential. In addition, the formation of such complex structure is found to be accompanied by the coherence revival phenomena.

2. Theoretical analysis

Let us focus on the dynamic evolution of a two-dimensional (2D) condensate driven by a time-dependent (anisotropic) harmonic potential $V(\mathbf{r}) = m \sum_u \omega_u^2 r_u^2 / 2$ with $u = x, y$. The corresponding dynamics of the system is described by the Gross–Pitaevskii equation (GPE)

$$i\hbar \frac{\partial \psi}{\partial t} = -\frac{\hbar^2}{2m} \Delta \psi + \left[\frac{m}{2} \sum_u \omega_u^2(t) r_u^2 + U|\psi|^2 \right] \psi, \quad (1)$$

where $\psi(\vec{r}, t)$ is the normalized wavefunction satisfying $\int d\mathbf{r} \psi^\dagger \psi = 1$. For convenience, we take natural units of length and energy as $a_0 = \sqrt{\hbar/m\omega_0}$ and $E_\omega = \hbar\omega_0$ respectively, with $\omega_0 = \omega_x(0) = \omega_y(0)$ being the initial isotropic harmonic frequency. The GPE then can be written in the dimensionless form

$$i \frac{\partial \tilde{\psi}}{\partial \tilde{t}} = \left(-\frac{1}{2} \Delta + \frac{1}{2} \sum_u A_u(t) \tilde{r}_u^2 + \beta |\tilde{\psi}|^2 \right) \tilde{\psi}, \quad (2)$$

where $\tilde{\psi} = a_0 \psi$, $\tilde{r}_u = r_u/a_0$, $\tilde{t} = \omega_0 t$, $A_u(t) = \omega_u^2(t)/\omega_0^2$, and $\beta = U/(a^2 \hbar \omega_0)$. In the following, the tilde is omitted without losing the physical properties.

2.1. Absence of inter-particle interaction

Considering an ideal Bose gas without any inter-particle interactions (i.e. $\beta = 0$), the dynamics of the condensate along the x - and y - directions are completely decoupled from each other. The total Hamiltonian can be written as $H(t) = \sum_u H_u$, where

$$H_u(t) = \left(\frac{1}{2} \hat{p}_u^2 + \frac{1}{2} A_u(t) \hat{q}_u^2 \right) = (\hat{k}_u^+ + A_u(t) \hat{k}_u^-) \quad (3)$$

with $\hat{k}_u^+ = \hat{p}_u^2/2$, $\hat{k}_u^- = r_u^2/2$ and $\hat{k}_u^0 = -i(\hat{p}_u r_u + r_u \hat{p}_u)/4$ being the operators of the $SU(1, 1)$ algebra, satisfying $[\hat{k}_u^+, \hat{k}_u^-] = 2\delta_{uv} \hat{k}_u^0$ and $[\hat{k}_u^0, \hat{k}_u^\pm] = \pm \delta_{uv} \hat{k}_u^\pm$. By performing the gauge transformation $\hat{U}(t) = \exp(i \sum_u v_u^-(t) \hat{k}_u^-) \exp(\sum_u v_u^0(t) \hat{k}_u^0)$ under the best gauge conditions

$$2v_u^- - v_u^0 = 0, \exp(2v_u^0)[(v_u^-)^2 + A_u(t) + v_u^-] = 1, \quad (4)$$

the Hamiltonian transforms into [39]

$$\bar{H} = U^{-1} \hat{H} U - iU^{-1} \frac{\partial U}{\partial t} = \sum_u f_u(t) \left(\frac{1}{2} \hat{p}_u^2 + \frac{1}{2} \hat{q}_u^2 \right),$$

where $f_u(t) = \exp(-v_u^0(t))$. The instantaneous gauged ground state of \bar{H} is easily derived as

$$\bar{\psi}(r_u, t) = \sqrt{\frac{1}{\pi}} \exp(-i \sum_u \theta_u(t)) \exp(-\frac{1}{2} \sum_u r_u^2), \quad (5)$$

where $\theta_u(t) = -\int_0^t f_u(\tau) d\tau/2$. Correspondingly, the exact solution of the origin Hamiltonian $H(t)$ with the time-dependent potential can be found,

$$\psi(r_u, t) = \sqrt{\frac{1}{\pi \prod_u \chi_u(t)}} \exp \left[-i \sum_u \theta_u(t) + \sum_u \frac{i}{2} v_u^- r_u^2 \right] \exp \left[-\frac{1}{2} \sum_u r_u^2 / \chi_u(t) \right] \quad (6)$$

with $\chi_u(t) = \exp(v_u^0(t)/2)$. From the equation (6), one can see that under the influence of the time-dependent harmonic potential, the wavefunction of the ideal Bose gas includes a dynamic phase $\sum_u (v_u^- r_u^2)/2$. The spatial distribution of density becomes time-dependent as well, and its width is modulated by $\chi_u(t)$.

Taking into account gauge conditions in equation (4), the equation of motion of $\chi_u(t)$ can be written as,

$$\ddot{\chi}_u = \frac{1}{\chi_u^3} - A_u(t)\chi_u, \quad (7)$$

which determines the time evolution of the density distribution. Note that the dynamic parameter v_u^- depends on $\chi_u(t)$ through the relationship $v_u^- = \dot{\chi}_u/\chi_u$. Therefore, the density and phase dynamics are not independent but bound to each other even without any inter-particle interactions.

2.2. Presence of inter-particle interaction

If the inter-particle interaction is taken under consideration, the system becomes highly nonlinear, and the above algebraic dynamic approach is no longer applicable. However, if the BEC is in the hydrodynamic limit, the system preserves the intrinsic conformal symmetry [21, 22, 32]. Using the scaling approach and introducing the scaling parameter $b_u(t)$ gives the solution of the condensate in the following form [24–26]

$$\psi = \mathcal{V}^{-1/2}(t)\xi_0(d_u, \tau(t))\exp[i\phi(\mathbf{r}, t)] \quad (8)$$

where $d_u = r_u/b_u(t)$, the dimensionless volume $\mathcal{V}(t) = \prod_u b_u(t)$ and $\tau(t) = \int^t dt'/\mathcal{V}(t')$. The phase is given by $\phi(\mathbf{r}, t) = \sum_u r_u^2 [\dot{b}_u(t)/2b_u(t)]$, which is very similar to the dynamic phase in equation (6). In other words, the scaling parameter b_u plays the same role as $\chi_u(t)$ in the ideal Bose gas limit. Furthermore, here, b_u is determined by the self-consistent equation

$$\ddot{b}_u + A_u(t)b_u = 1/(b_u\mathcal{V}(t)), \quad (9)$$

which takes similar form of the equations of motion of $\chi_u(t)$ (equation (7)). It is clear that the induced time modulations of the density (described by b_u) and the phase (determined by $\dot{b}_u/b_u(t)$) are ultimately coupled to each other in the condensate with finite inter-particle interactions.

Given the initial conditions $b_u(0) = 1$, $\dot{b}_u(t) = 0$, we get the dynamic equation of ξ_0 [25]

$$i\frac{\partial \xi_0}{\partial \tau} = -\frac{1}{2} \sum_u \frac{\mathcal{V}(t)}{b_u^2(t)} \Delta \xi_0 + \frac{1}{2} \sum_u d_u^2 \xi_0 + \beta |\xi_0|^2 \xi_0. \quad (10)$$

In the Thomas–Fermi limit, an universal scaling solution reads

$$\xi_0(d_u, \tau(t)) = \frac{1}{\beta} \left(\mu - \frac{1}{2} \sum_u \frac{r_u^2}{b_u^2(t)} \right)^{1/2} \exp(-i\mu\tau(t)), \quad (11)$$

where μ is the chemical potential. The dynamics of BECs is then described by the equations (8), (9), and (11).

3. Numerical simulations

According to the above theoretical analysis, when the system is driven by the time-dependent harmonic trapping potential, the condensate wavefunction includes an extra dynamic phase, no matter if there is the inter-particle interaction or not. Such a dynamic phase quadratically depends on the position r_u and may lead to decoherence effects. Moreover, because \dot{b}_u/b_u ($\dot{\chi}_u/\chi_u$) varies with time, it could also exert further influence on the decoherence process. These combined spatiotemporal oscillations of the dynamic phase may produce significant phase fluctuations in the dynamic evolution process [19]. However, both the algebraic dynamic approach and the scaling method can only give a consistent description for the overall density profile of the condensate, the detailed structure and internal fluctuation evaluation are beyond their capabilities and the use of quantitative numeric methods is required.

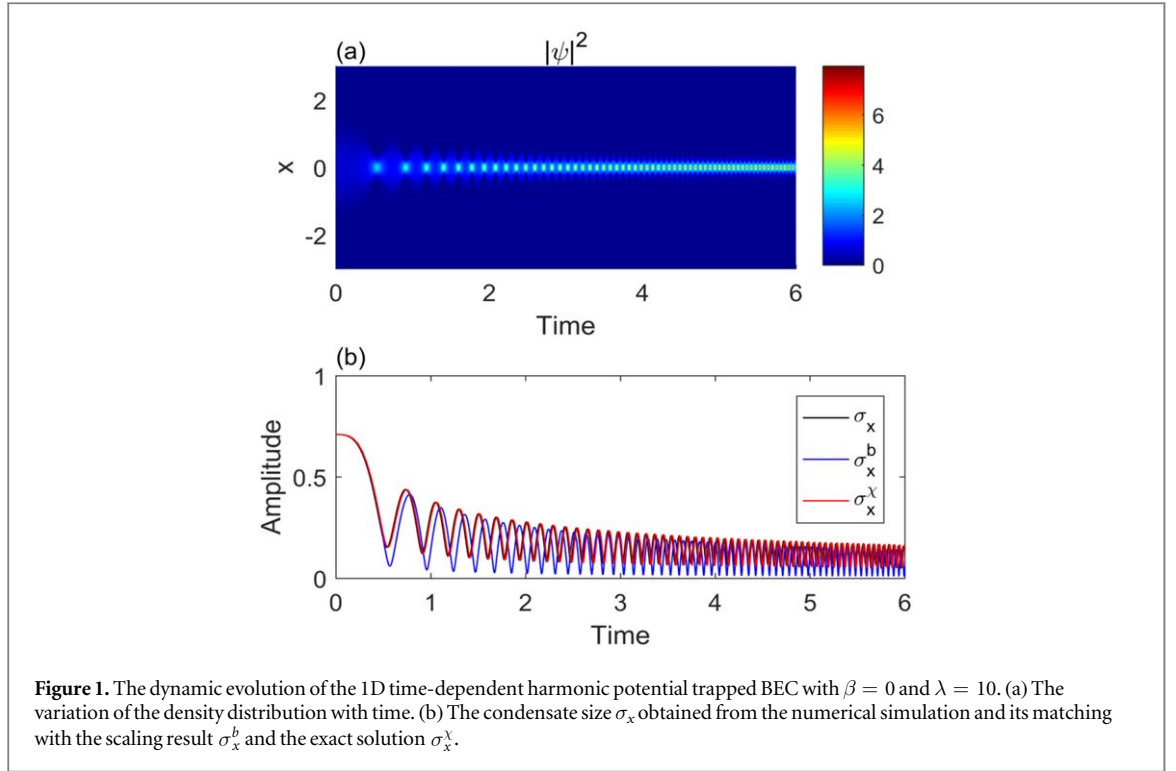
The coherent property of the condensate is directly linked to the long range off-diagonal order of BEC [42], which can be inferred from the spatial correlation function [7, 8, 20, 43–45]

$$\mathcal{C}(r) = [\psi(0)^*\psi(r) + \psi(r)^*\psi(0)]/2. \quad (12)$$

Clearly, the phase decoherence will result in random spatial fluctuations of $\mathcal{C}(r)$. For the (coherent) ideal Bose gas, described by equation (6), the correlation function reads,

$$\mathcal{C}(r) = \frac{1}{\sqrt{\pi}\chi_x} \exp(-x^2/2\chi_x^2) \cos(v_x^- x^2/2) \quad (13)$$

which is determined by the spatial distribution of density and the extra dynamic phase through the parameters χ_x and v_x^- , respectively. On the other hand, in the strong inter-particle interaction limit, with the scaling solution equation (11), the correlation function is given by



$$\mathcal{C}(r) = \frac{1}{\beta^2 \mathcal{V}} \sqrt{\mu \left(\mu - \frac{1}{2} \sum_u \frac{r_u^2}{b_u^2(t)} \right)} \cos(\phi) \quad (14)$$

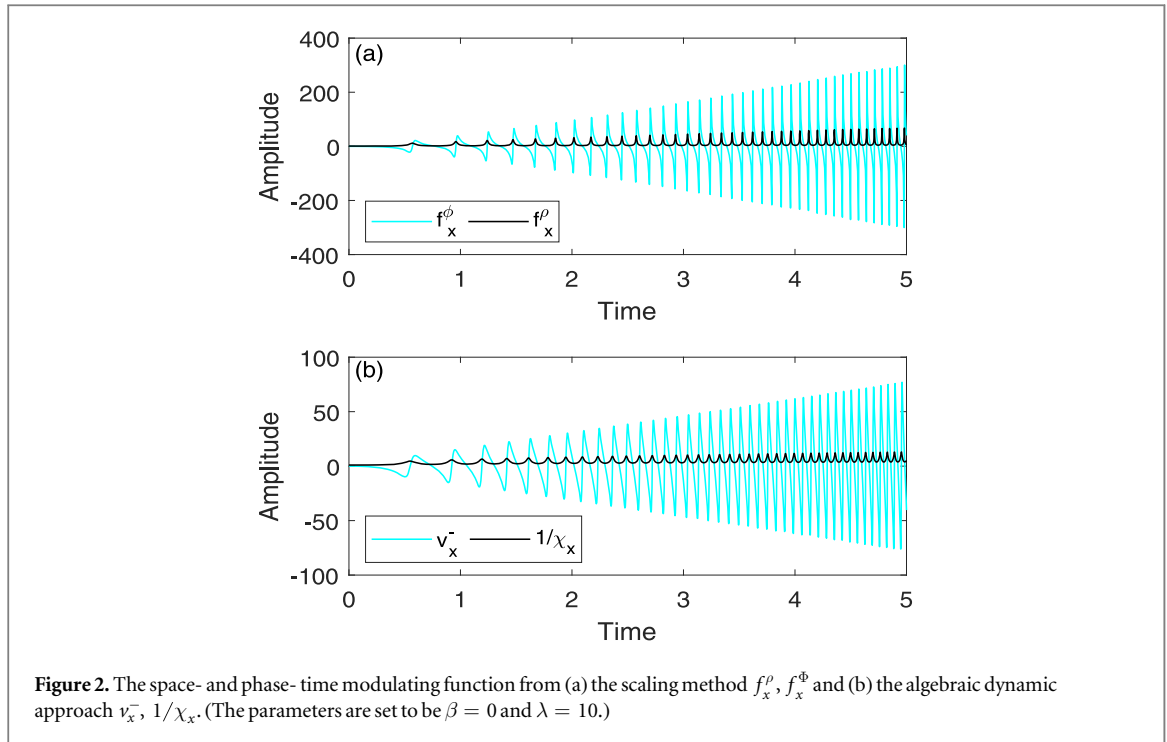
which is given by the chemical potential and the dynamic phase ϕ . In addition, in the following, we will trace the dynamic evolution of the amplitude and the phase through two well-defined functions $f_u^\rho(t) = 1/b_u(t)$ and $f_u^\phi(t) = \dot{b}_u(t)/(2b_u(t))$, respectively.

3.1. One-dimensional (1D) BEC

For better understanding of the dynamic phenomenon in BECs, the 1D condensate was investigated firstly. To induce phase fluctuations in 1D system, the trapping potential parameter $A_x(t)$ is set to increase with time, $A_x = (1 + \lambda t)^2$, where λ is the tunable speed parameter.

The time evolution of BECs is obtained by introducing $A_x(t)$ into equations (4), (7), and (9). For comparison, a better quantitative description of BEC dynamics is provided by numerically solving the GPE via the well-developed GPESLab [40, 41]: firstly, the ground state of the system is obtained with the imaginary time method [41], then with the time-splitting scheme [40], the dynamic evolution of the system driven by the time-dependent trapping potential is determined. Numerically, the expected value $\langle \sigma_x^2 \rangle$ of x^2 is used to characterize the density dynamics, $\sigma_x^2 = \int \psi^* x^2 \psi dx$.

The variation of density distribution with time is shown in figure 1(a) and the parameters used in the simulation were set as follows: $\beta = 0$, $\lambda = 10$. For better quantitative comparison, by multiplying the parameter b_x and χ_x with the initial condensate size $\sigma_x(0)$, the condensate size predicted by the scaling method and the algebraic dynamic approach can be obtained: $\sigma_x^b = b_x \sigma_x(0)$, $\sigma_x^x = \chi_x \sigma_x(0)$. Figure 1(b) shows the numeric condensate size σ_x together with the analytical result σ_x^b and σ_x^x . As demonstrated in figure 1, in the case of BEC without inter-particle interaction ($\beta = 0$), the exact solution σ_x^x oscillates with the amplitude reducing and the frequency increasing gradually. Furthermore, both the condensate size σ_x (from numeric simulation) and the scaling result σ_x^b give correct predictions of the oscillation behavior, confirming, thus, the validity of the GPESLab and the scaling method. On the other hand, one can see that while the oscillation behavior of σ_x^x is perfectly synchronized with σ_x , the scale parameters σ_x^b shows a little phase mismatch and amplitude decrease comparing with σ_x , due to the difference in equations of motion used. Figures 2(a) and (b) demonstrate the dynamic evolution of space- and phase- time modulating functions f_x^ρ , f_x^ϕ , as obtained from the scaling method, and $1/\chi_x$, ν_x^- in algebraic dynamic approach, respectively. From the figures, it is obvious that both the scaling method and the algebraic dynamic approach give similar results; the space- and phase- time modulating functions are fully synchronized with f_x^ϕ (ν_0^-), which changes abruptly at the peak of f_x^ρ ($1/\chi_x$). As can be seen in figure 1(a), even with such an abrupt phase variation, the condensate only oscillates with time and no signature of the phase decoherence is observed. This behavior can be explained by the sound velocity in BEC, which is



directly linked to the inter-particle interaction $c = \sqrt{\beta n}$ [42] (n is the particle density), and sets up the upper limitation for the speed of information exchange in the condensate. In the absence of the inter-particle interaction, the sound velocity in condensate is zero. Hence, the dynamics in different locations is uncorrelated and controlled only by the external time-dependent potential, as results from the correlation function equation (13). The wavefunction of the system is well described by the solution of equation (6) in the algebraic dynamic approach, which is exact and coherent all the time. Thus, the system changes adiabatically under the drive of trapping potential, the coherent property of the condensate is preserved and the changes in the condensate phase do not cause any fluctuations in the density distribution.

When the strength of the inter-particle interaction is non-zero, the condensate size is again modulated by parameter b_x (equation (9)) and the time variations in the space- and phase- modulating functions f_x^ρ, f_x^ϕ are also same as in the non-interacting case (see figure 2(a)). But the presence of the inter-particle interaction makes the condensate dynamics in different positions correlated and the abrupt phase variation can lead to changes in the density distribution.

For the inter-particle interaction strength $\beta = 100$, variations in the density distribution and condensate width with time are shown in figures 3(a) and (b), respectively. From figure 3(b), one can see that the variations of condensate size σ_x and the scaling result σ_x^b are synchronized in the early stage. But starting around $t = 3$, there is a great discrepancy between σ_x and σ_x^b and the amplitude variation of σ_x is much smaller than σ_x^b , which indicates that the system radically changes from the hydrodynamic limit and goes beyond the scaling method description.

Figure 4 shows the condensate density distributions (black line) and the corresponding spatial correlation (red line) $\mathcal{C}(x)$ at different times $t = 0.0, 1.63, 1.70, 1.97, 2.03, 5.50$. As can be seen in the figures, the spatial correlation profiles not only overlap with the density distribution lines, but also contain the additional phase distribution information, from which the phase fluctuations can be determined. In contrast to the non-interacting particle case, where the phase variation does not affect the condensate density distribution, the inter-particle interaction leads to the phase dispersion across the condensate, which would give rise to the additional phase fluctuations and interference effects in the system. Because the dynamic phase quadratically depends on x , it will increase faster further away from the center of the condensate. Therefore, under the influence of the phase-time modulating function f_x^ϕ , in the contraction process, the wide phase variations at the edges of the condensate quickly disperse inwardly and multi-phase modes accumulate in the condensate. Due to these process, the phase of the condensate will be disturbed by the multi-peak structure arising at the edges of the condensate and subsequently moving towards the center of the condensate. From figure 4, it is obvious that the distinct phase fluctuations arise in the condensate at $t = 1.63, 1.97$. On the other hand, in the expanding process, the phase variations move outwards and the correlation function follows the proposed model and varies smoothly; no observable phase fluctuations emerge ($t = 1.7$ and 2.03). In addition, the phase-time modulating

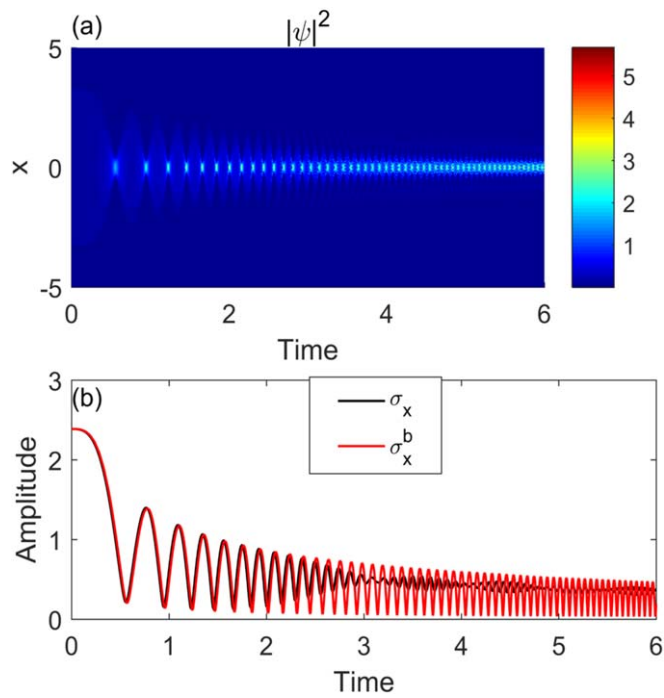


Figure 3. (a) Multi-peak structure of the density distribution of the 1D Bose–Einstein condensate for the interaction strength $\beta = 100$. (b) The condensate size σ_x , which for $\beta = 100$ deviates from the scaling result σ_x^b in long time.

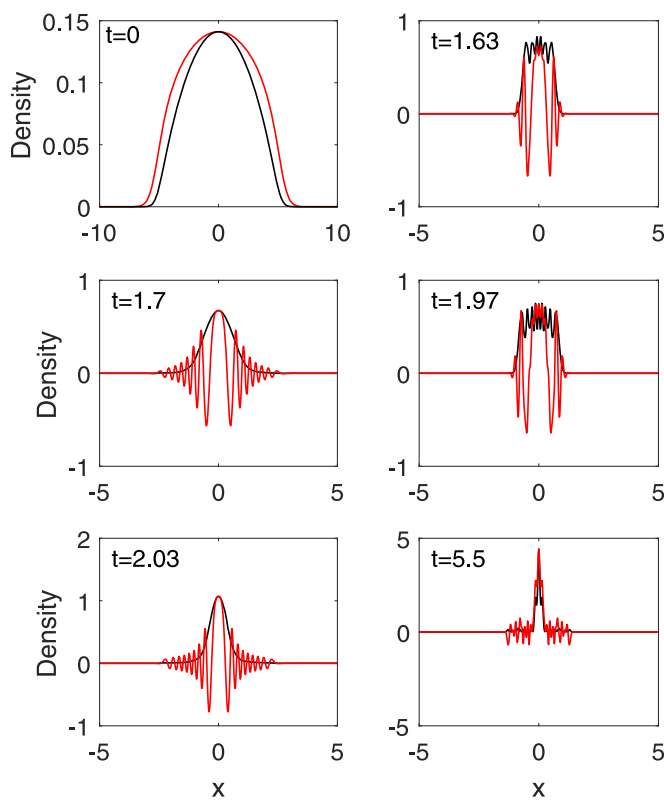
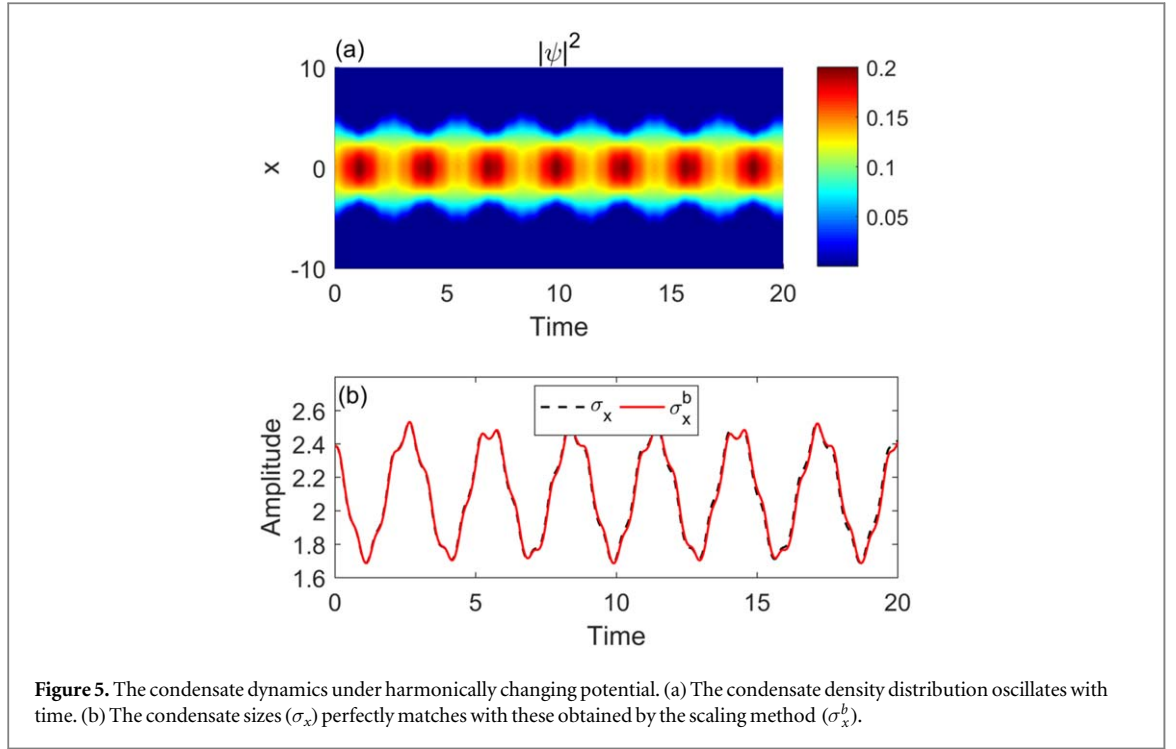


Figure 4. The condensate density distribution (black line) and the corresponding spatial correlation function (red line) at different times $t = 0.0, 1.63, 1.70, 1.97, 2.03, 5.50$ with parameter $\beta = 100$, and $\lambda = 10$.



function f_x^ϕ changes from negative value in the contraction process to positive value in the expanding process. At zero point, the coherence property of the system can revive [19], and so the phase coherence of the condensate reemerges in the expanding process. However, in the long-time simulation (figure 4, $t = 5.50$), a chaotic motion may occur in the system due to the accumulation of the phase and density fluctuations.

When the trapping frequency changes harmonically in time, instead of increasing the trapping potential frequency linearly, the condensate oscillates with time following the variations in frequency. In figure 5, the trapping frequency of 1D condensate was changed harmonically with $A_x = (1 + \sin(10t))^2$. It is shown that the condensate remains coherent at all the investigated times, the variation of the condensate size can be well described by the scaling method, and there is no signature of the density or phase fluctuations. For 2D and 3D cases, the obtained results are similar to these of the 1D case: no phase fluctuations and multi-peak structure are observed and the time evolution of condensate is consistent with the scaling method if the trapping potential changes harmonically in time.

3.2. 2D BEC

Due to the restriction of the 1D system, the phase fluctuation signature and the phase revival behavior cannot sustain for long time. In order to stabilize these effects, a less restricted system, i.e. a 2D time-dependent harmonic potential trapped BEC is considered. To induce phase fluctuations in this system, we increase the frequency of harmonic trap in the x direction and keep the y direction unchanged, this leads to $A_x = (1 + \lambda t)^2$, $A_y = 1$.

In the absence of the inter-particle interaction, the system dynamics along different directions are decoupled. Since the frequency of the harmonic trapping potential only changes along x axis, the condensate dynamics is restricted in the x direction, which makes the system an effective 1D system similar to the system discussed in previous section. The condensate remains coherent all the time with the width along the x direction varying with time identically as in the 1D case (figure 1(b)), the space- and phase- time modulating functions are also synchronized, resembling the 1D case (figure 2).

In contrast to the ideal Bose gas limit, the presence of the inter-particle interaction as an origin of nonlinear-type interactions would lead to the coupling of dynamics along different directions, as demonstrated in equation (9). Then, the time-dependent harmonic potential along the x direction not only drives particles to move around in the x direction, but also exerts a non-trivial influence on the dynamics along the y direction. The dynamic equation (9) become as follows:

$$\begin{aligned}\ddot{b}_x &= -(1 + \lambda t)^2 b_x + 1/(b_x^2 b_y), \\ \ddot{b}_y &= -b_y + 1/(b_y^2 b_x).\end{aligned}\tag{15}$$

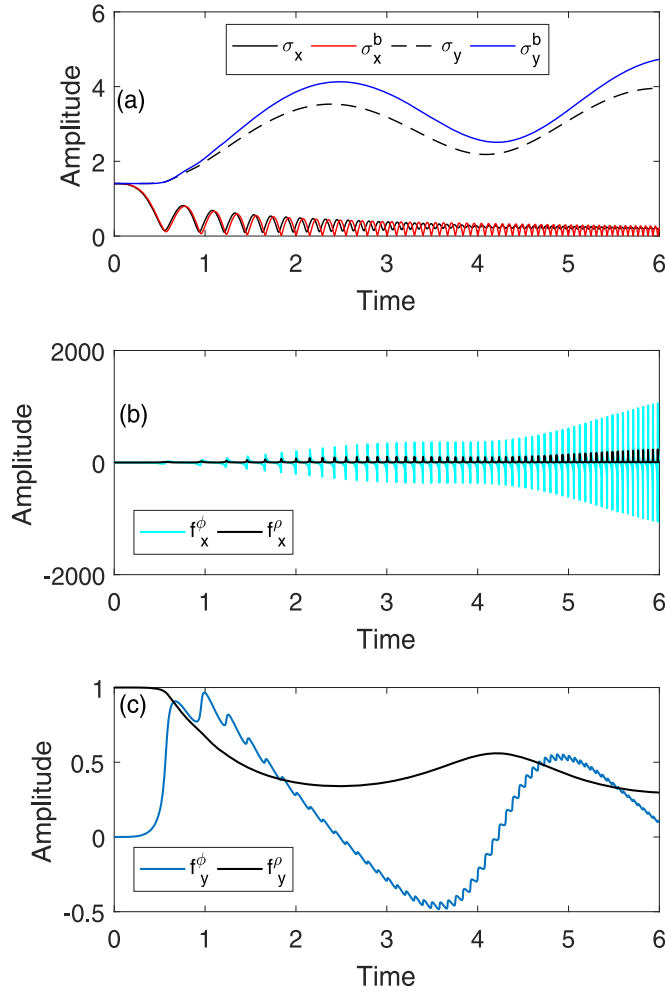


Figure 6. (a) The condensate density oscillation for the inter-particle interaction strength $\beta = 100$. The oscillation matches well with the scale result in the x and y directions. (b) The space- and phase- time modulating function f_x^ρ, f_x^ϕ respectively, in the x direction. The functions are well synchronized. (c) The space- and phase- time modulating function f_y^ρ, f_y^ϕ along the y direction. The functions are synchronized poorly. In addition, the f_y^ϕ function includes the phase fluctuations.

By solving the coupled equations in equation (15), the corresponding variation of the scaling parameters b_x, b_y can be obtained. In our numerical calculations, the interaction strength was set to $\beta = 100$. As one can see in figure 6(a), by including the inter-particle interaction, both the condensate size σ_x and σ_y oscillate with time. Comparing with the scaling results $\sigma_x^b = b_x \sigma_x(0)$ and $\sigma_y^b = b_y \sigma_y(0)$, the variation in the condensate size is well described by the scaling method. Along the x direction, σ_x and σ_x^b are synchronized, while in the y direction, σ_y is smaller than the scaling method predicted value σ_y^b .

Figures 6(b) and (c) show the variation of space- and phase- time modulating functions along the x and y directions. From the figures, it is clear that both the functions along the x direction f_x^ρ, f_x^ϕ are well synchronized with their wave shapes modulated by the coupling with the y direction, while as those along the y direction f_y^ρ, f_y^ϕ are roughly synchronized, and in addition, the phase modulating function f_y^ϕ is accompanied with fluctuations. Thus, the variation in BEC induced by the time-dependent potential in the x direction is transferred to the y direction by the nonlinear interaction. On the other hand, the presence of the inter-particle interaction makes the condensate dynamics in different positions correlated. Taking into account all these effects, the system under the fast varying trapping potential is expected to change non-adiabatically and the abrupt phase variations in the x direction and the phase fluctuations in the y direction would lead to considerable changes in the density distribution and, thus, disrupt the coherence property of the system.

Figure 7 illustrates the numerically simulated condensate density distribution and the corresponding spatial correlation functions at different times $t = 0, 1.78, 1.90, 0.91, 2.72$, and 5.5 . As can be seen from the figure, the system not only shows the oscillations of the density distribution with time, but also takes on the multi-peak structure along both the x and y directions in the evolving process. Such behavior is similar to that in the 1D case. Thus, the large phase variation induced by the time-dependent trapping potential causes the phase fluctuations and the decoherence effect along the x direction, and concurrently through the nonlinear coupling, same

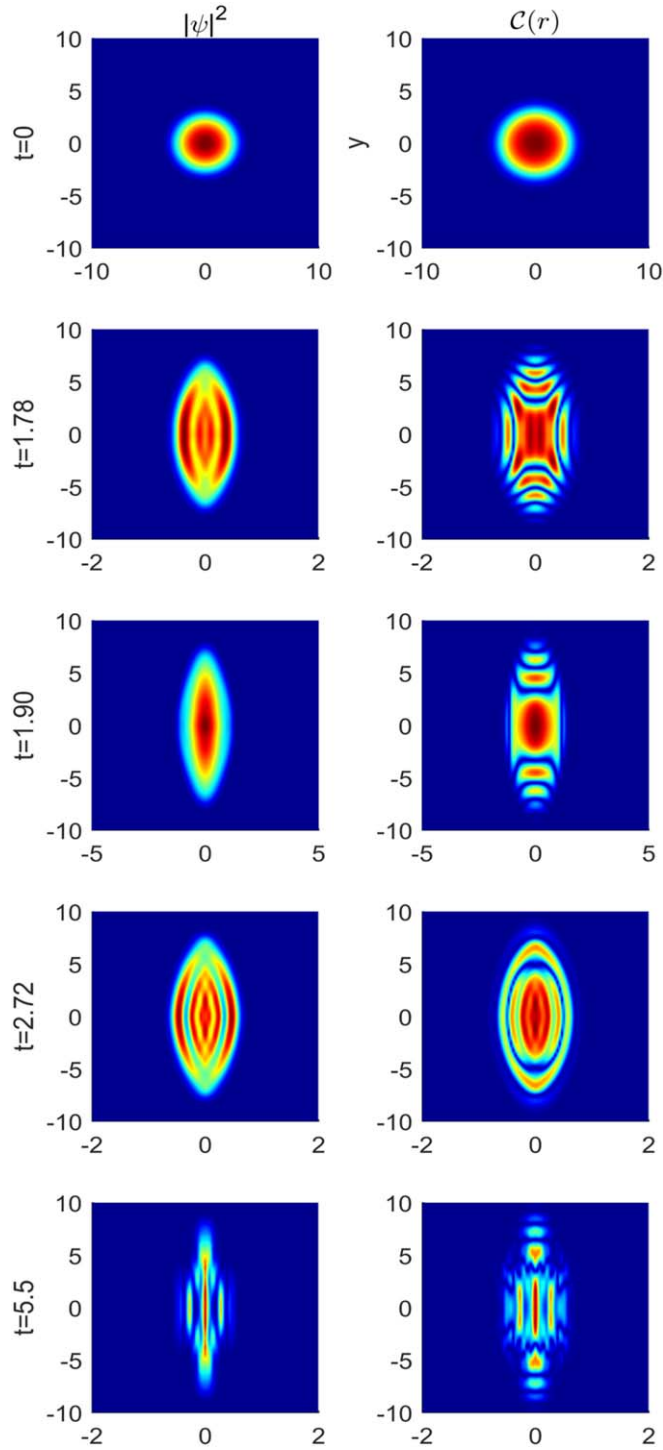


Figure 7. The condensate density distribution and the corresponding spatial correlation function of the 2D BECs at different times $t = 0, 1.78, 1.90, 0.91, 2.72$ and 5.5 ($\beta = 100, \lambda = 10$).

behavior can also be transferred into the y direction. Furthermore, a revival of the coherence can be observed along the x, y directions at the same time, confirming the phase fluctuations and the decoherence effect being induced by the variation of the time-dependent trapping potential. In contrast to the 1D case, the 2D BEC with the inter-particle interaction is less restricted. Hence, the influence exerted by the time-dependent potential, which can be transferred to the other direction, makes the above mentioned phase fluctuations, the decoherence effect and the coherence revival behavior more stable and suitable for observation. However, in the longer time simulation, the undesirable additional excitations and chaotic motion may occur in the system.

For experimentally feasible 3D case, we obtained similar results. Starting with an initial 3D isotropic harmonic trap, we changed the harmonic potential frequency along the z direction by $A_z = (1 + \lambda t)^2$ with $\lambda = 10$ and kept the frequencies along the x and y directions unchanged. Because of less dimensional restriction,

the 3D case is found to be more stable, the related density and phase fluctuations, phase coherence revival phenomena are similar to these of the 2D case but the phase coherence can be maintained for much longer time. Furthermore, due to the isotropy in the xy plane, the density distribution in the xy plane is accompanied by a formation of ring structures, similar to Newton rings in optics [33].

4. Conclusion

The dynamics of BECs under the time-dependent harmonic trapping potential was investigated. If there is no inter-particle interaction, the condensate remains coherent all the time with its density distribution oscillating in time. Even in the case of the strongly time-varied dynamic phase, no change in the density distribution of BEC was found. By employing both the algebraic dynamic approach and the scaling method, the oscillation behavior of BEC was successfully described. When the inter-particle interaction exists in the system, the sound velocity of the condensate becomes non-zero. The abrupt phase change produces considerable phase fluctuations in the system, which perturb and destroy the coherence property of the condensate. The occurrence of these fluctuations was further linked with the existence of the multi-peak structure of the density distribution. Because the dynamics phase induced by the time-dependent trapping potential can be zero at various time, the condensate was also found to exhibit the coherence revival behavior. In the 1D time-dependent trapped BEC, due to the low dimensional restriction, various modes and fluctuations are easily induced and populated with time, and may lead the system into chaotic motion very quickly. In the less-restricted 2D and 3D BECs, the dynamic characteristics along different directions are coupled together by the nonlinear interaction, making the system more stable and suitable for observation.

Acknowledgments

This work is supported by the National Natural Science Foundation of China (No.11474138 and No. 11834005), the German Research Foundation (No. SFB 762), the Program for Changjiang Scholars and Innovative Research Team in University (No. IRT-16R35), the Fundamental Research Funds for the Central Universities, Ministry of Science and Technology of China through grants CN-SK-8-4, the Slovak Academy of Sciences (VEGA Grant No. 2/0038/20) and the Slovak Research and Development Agency (APVV SK-CN-2017-0004).

ORCID iDs

Decheng Ma  <https://orcid.org/0000-0001-8955-1076>

Vladimir Koval  <https://orcid.org/0000-0003-2425-8738>

Chenglong Jia  <https://orcid.org/0000-0003-2064-923X>

References

- [1] Bongs K and Sengstock K 2004 *Rep. Prog. Phys.* **67** 907–63
- [2] Schumm T, Hofferberth S, Andersson L M, Wildermuth S, Groth S, Bar-Joseph I, Schmiedmayer J and Krüger P 2005 *Nat. Phys.* **1** 57–62
- [3] Mandel O, Greiner M, Widera A, Rom T, Hänsch T W and Bloch I 2003 *Nature* **425** 937–40
- [4] Micheli A, Jaksch D, Cirac J I and Zoller P 2003 *Phys. Rev. A* **67** 013607
- [5] Dettmer S et al 2001 *Phys. Rev. Lett.* **87** 160406
- [6] Mathey L, Ramanathan A, Wright K, Muniz S, Phillips W and Clark C 2010 *Phys. Rev. A* **82** 033607
- [7] Manz S et al 2010 *Phys. Rev. A* **81** 031610
- [8] Kadio D, Gajda M and Rządowski K 2005 *Phys. Rev. A* **72** 013607
- [9] Sinatra A and Castin Y 2008 *Phys. Rev. A* **78** 053615
- [10] Sinatra A, Castin Y and Witkowska E 2007 *Phys. Rev. A* **75** 033616
- [11] Hellweg D et al 2001 *Appl. Phys. B* **73** 781–9
- [12] de Leeuw A-W, Stoof H T C and Duine R A 2014 *Phys. Rev. A* **89** 053627
- [13] Ruschhaupt A, del Campo A and Muga J G 2006 *Eur. Phys. J. D* **40** 399–403
- [14] Graham R 1998 *Phys. Rev. Lett.* **81** 5262–5
- [15] Jo G-B, Choi J-H, Christensen C A, Lee Y-R, Pasquini T A, Ketterle W and Pritchard D E 2007 *Phys. Rev. Lett.* **99** 240406
- [16] Mazets I E 2012 *Phys. Rev. A* **86** 055603
- [17] Choi J, Seo S W, Kwon W J and Shin Y 2012 *Phys. Rev. Lett.* **109** 125301
- [18] Sklarz S E, Friedler I, Tannor D J, Band Y B and Williams C J 2002 *Phys. Rev. A* **66** 053620
- [19] Plata J 2004 *Phys. Rev. A* **69** 033604
- [20] Petrov D S, Shlyapnikov G V and Walraven J T M 2001 *Phys. Rev. Lett.* **87** 050404
- [21] Ghosh P K 2001 *Phys. Rev. A* **65** 012103
- [22] Gritsev V, Barmettler P and Demler E 2010 *New J. Phys.* **12** 113005
- [23] Schaff J-F, Capuzzi P, Labeyrie G and Vignolo P 2011 *New J. Phys.* **13** 113017

- [24] Castin Y and Dum R 1996 *Phys. Rev. Lett.* **77** 5315–9
- [25] Kagan Y, Surkov E L and Shlyapnikov G V 1997 *Phys. Rev. A* **55** R18–21
- [26] Kagan Y, Surkov E L and Shlyapnikov G V 1996 *Phys. Rev. A* **54** R1753–6
- [27] Vidanović I, Balaž A, Al-Jibbouri H and Pelster A 2011 *Phys. Rev. A* **84** 013618
- [28] Bruun G M and Clark C W 2000 *Phys. Rev. A* **61** 061601
- [29] Minguzzi A and Gangardt D M 2005 *Phys. Rev. Lett.* **94** 240404
- [30] Ripoll J J G and Pérez-García V M 1999 *Phys. Rev. A* **59** 2220–31
- [31] Castin Y and Dum R 1997 *Phys. Rev. Lett.* **79** 3553–6
- [32] Dalfovo F, Minniti C, Stringari S and Pitaevskii L 1997 *Phys. Lett. A* **227** 259–64
- [33] Kuznetsov E A, Kagan M Y and Turlapov A V 2019 arXiv:1903.04245
- [34] O'Hara K M 2002 *Science* **298** 2179
- [35] Ermakov P 2008 *Appl. Anal. Discrete Math.* **2** 1–25
- [36] Zakharov V E and Kuznetsov E A 2012 *Phys. Usp.* **55** 535–56
- [37] Mewes M-O, Andrews M R, van Druten N J, Kurn D M, Durfee D S and Ketterle W 1996 *Phys. Rev. Lett.* **77** 416
- [38] Pitaevskii L and Stringari S 2016 *Bose–Einstein Condensation and Superfluidity* (Oxford: Oxford University Press)
- [39] Wang S J, Zuo W, Weiguny A and Li F L 1994 *Phys. Lett. A* **196** 7–12
- [40] Antoine X and Duboscq R 2015 *Comput. Phys. Commun.* **193** 95–117
- [41] Antoine X and Duboscq R 2014 *Comput. Phys. Commun.* **185** 2969–91
- [42] Dalfovo F, Giorgini S, Pitaevskii L P and Stringari S 1999 *Rev. Mod. Phys.* **71** 463–512
- [43] Proukakis N P 2006 *Phys. Rev. A* **74** 053617
- [44] Petrov D S, Shlyapnikov G V and Walraven J T M 2000 *Phys. Rev. Lett.* **85** 3745–9
- [45] Henkel C, Sauer T-O and Proukakis N P 2017 *J. Phys. B: At. Mol. Opt. Phys.* **50** 114002